

Creation of multi-frequency terahertz waves by optimized cascaded difference frequency generation

Zhong-Yang Li(李忠洋), Jia Zhao(赵佳), Sheng Yuan(袁胜), Bin-Zhe Jiao(焦彬哲), Pi-Bin Bing(邴丕彬), Hong-Tao Zhang(张红涛), Zhi-Liang Chen(陈治良), Lian Tan(谭联), and Jian-Quan Yao(姚建铨)

Citation: Chin. Phys. B, 2022, 31 (**4**): 044205. DOI: 10.1088/1674-1056/ac29b4
Journal homepage: http://cpb.iphy.ac.cn; http://iopscience.iop.org/cpb

What follows is a list of articles you may be interested in

High-efficiency terahertz wave generation with multiple frequencies by optimized cascaded difference frequency generation

Zhongyang Li(李忠洋), Binzhe Jiao(焦彬哲), Wenkai Liu(刘文锴), Qingfeng Hu(胡青峰), Gege Zhang(张格格), Qianze Yan(颜钤泽), Pibin Bing(邴丕彬), Fengrui Zhang(张风蕊), Zhan Wang(王湛), and Jianquan Yao(姚建铨)
Chin. Phys. B, 2021, 30 (**4**): 044211. DOI: 10.1088/1674-1056/abe3eb

Theoretical research on terahertz wave generation from planar waveguide by optimized cascaded difference frequency generation

Zhongyang Li(李忠洋), Jia Zhao(赵佳), Wenkai Liu(刘文锴), Qingfeng Hu(胡青峰), Yongjun Li(李永军), Binzhe Jiao(焦彬哲), Pibin Bing(邴丕彬), Hongtao Zhang(张红涛), Lian Tan(谭联), and Jianquan Yao(姚建铨)
Chin. Phys. B, 2021, 30 (**2**): 024209. DOI: 10.1088/1674-1056/abc3b7

Guiding properties of proton-implanted Nd^{3+}-doped phosphate glass waveguides

Qi-Feng Zhu(朱其峰), Yue Wang(王玥), Jian-Ping Shen(沈建平), Hai-Tao Guo(郭海涛), Chun-Xiao Liu(刘春晓)
Chin. Phys. B, 2018, 27 (**5**): 054218. DOI: 10.1088/1674-1056/27/5/054218

Planar waveguides in neodymium-doped calcium niobium gallium garnet crystals produced by proton implantation

Chun-Xiao Liu(刘春晓), Meng Chen(陈梦), Li-Li Fu(付丽丽), Rui-Lin Zheng(郑锐林), Hai-Tao Guo(郭海涛), Zhi-Guang Zhou(周志广), Wei-Nan Li(李玮楠), She-Bao Lin(林社宝), Wei Wei(韦玮)
Chin. Phys. B, 2016, 25 (**4**): 044211. DOI: 10.1088/1674-1056/25/4/044211

Optical planar waveguides in Yb^{3+}-doped phosphate glasses produced by He^{+} ion implantation

Liu Chun-Xiao, Li Wei-Nan, Wei Wei, Peng Bo
Chin. Phys. B, 2012, 21 (**7**): 074211. DOI: 10.1088/1674-1056/21/7/074211

Creation of multi-frequency terahertz waves by optimized cascaded difference frequency generation

Zhong-Yang Li(李忠洋)[1,†], Jia Zhao(赵佳)[1], Sheng Yuan(袁胜)[1], Bin-Zhe Jiao(焦彬哲)[1], Pi-Bin Bing(邴丕彬)[1], Hong-Tao Zhang(张红涛)[1], Zhi-Liang Chen(陈治良)[1], Lian Tan(谭联)[1], and Jian-Quan Yao(姚建铨)[2]

[1] *College of Electric Power, North China University of Water Resources and Electric Power, Zhengzhou* 450045, *China*
[2] *College of Precision Instrument and Opto-electronics Engineering, Institute of Laser and Opto-electronics, Tianjin University, Tianjin* 300072, *China*

(Received 15 July 2021; revised manuscript received 13 September 2021; accepted manuscript online 24 September 2021)

A new scheme which generates multi-frequency terahertz (THz) waves from planar waveguide by the optimized cascaded difference frequency generation (OCDFG) is proposed. A THz wave with frequency ω_{T1} is generated by the OCDFG with two infrared pump waves, and simultaneously a series of cascaded optical waves with a frequency interval ω_{T1} is generated. The THz wave with a frequency of M-times ω_{T1} is generated by mixing the m-th-order and the $(m+M)$-th-order cascaded optical wave. The phase mismatch distributions of cascaded difference frequency generation (CDFG) are modulated by changing the thickness of planar waveguide step by step, thereby satisfying the phase-matching condition from first-order to high-order cascaded Stokes process step by step. As a result, the intensity of THz wave can be enhanced and modulated by controlling the cascading order of OCDFG.

Keywords: multi-frequency terahertz wave, optimized cascaded difference frequency generation, planar waveguide

PACS: 42.65.Yj, 42.65.Dr, 42.65.Ky **DOI:** 10.1088/1674-1056/ac29b4

1. Introduction

Owing to wide applications of terahertz (THz) wave in security inspection, military radar detection, medical imaging, and non-destructive inspection,[1–4] how to generate high-efficiency multi-frequency THz waves becomes the focus of attention. Compared with other THz wave generation methods, cascaded difference frequency generation (CDFG) can effectively improve the conversion efficiency of THz wave.[5–11] However, the phase-matching conditions of each order cascaded Stokes process are different. As the cascading order increases, the phase mismatches gradually become larger, which restrains the energy transformation from pump wave to high-order Stokes waves. Moreover, the reported CDFG can only generate the THz wave with a fixed frequency because the frequency interval between the two input infrared lasers is fixed.[10,11] If the m-th-order and the $(m+M)$-th-order cascaded optical wave which generates in CDFG, efficiently interact with each other, the THz waves with multi-frequency can be produced by only two fixed frequency laser.

In this work, we propose an innovative scheme to generate multi-frequency THz waves by the optimized cascaded difference frequency generation (OCDFG) in a planar waveguide. By optimizing the phase mismatch distributions of CDFG, the pump photons are transferred to high-order Stokes waves, resulting in a high-efficiency THz wave generation. By enhancing the interaction between the m-th-order optical wave and the $(m+M)$-th-order optical wave, the multi-frequency THz waves are realized.

2. Theoretical model

Figure 1(a) shows the schematic diagram of generating multi-frequency terahertz waves in accordance with the basic principle of CDFG. In the schematic diagram, the black two-way arrow curves indicate that each cascaded optical wave can interact with any other cascaded optical waves, so that the THz wave with multi-frequency can be generated. The phase-matching condition of the first-order CDFG in a planar waveguide is given by the following equation:[12]

$$\frac{n_{\rm p}}{\lambda_{\rm p}} - \frac{n_{\rm s}}{\lambda_{\rm s}} = \frac{n_{\rm eff,THz}}{\lambda_{\rm T}}, \tag{1}$$

where n and λ represent the refractive index and wavelength respectively, the subscripts p, s, and T denote the pump wave, signal wave, and THz wave respectively. $n_{\rm eff,THz}$ refers to the effective refractive index of fundamental TM-mode THz wave.

The input pump wave (ω) and the first-order Stokes wave (ω_1) generate the THz wave ($\omega_{T1} = \omega_0 - \omega_1$) by difference frequency generation (DFG). By changing THz wave effective refractive index $n_{\rm eff,THz}$ to satisfy the phase-matching conditions between the m-th-order and the $(m+1)$-th-order cascaded optical waves, a series of cascaded optical waves (ω_m) with an interval of ω_{T1} and THz wave (ω_{T1}) are generated.

[†]Corresponding author. E-mail: thzwave@163.com

© 2022 Chinese Physical Society and IOP Publishing Ltd

By changing THz wave effective refractive index $n_{\mathrm{eff,THz}}$ to satisfy the phase-matching conditions between the m-th-order and the $(m+2)$-th-order cascaded optical waves, the THz wave with a frequency of ω_{T2} ($\omega_{\mathrm{T2}} = 2 \times \omega_{\mathrm{T1}}$) is generated. Similarly, $n_{\mathrm{eff,THz}}$ can satisfy the phase-matching conditions between the m-th-order and the $(m+M)$-th-order cascaded optical waves, resulting in the THz wave generation with a frequency of $\omega_{\mathrm{T}M}$ ($\omega_{\mathrm{T}M} = M \times \omega_{\mathrm{T1}}$). The relationship between $n_{\mathrm{eff,THz}}$ of fundamental TM-mode THz wave and the thickness of planar waveguide t is expressed as[12]

$$\frac{t}{\lambda_{\mathrm{T}}} = \frac{1}{\pi\sqrt{n_{\mathrm{T}}^2 - n_{\mathrm{eff,THz}}^2}} \tan^{-1}\left(n_{\mathrm{T}}\sqrt{\frac{n_{\mathrm{eff,THz}}^2 - 1}{n_{\mathrm{T}}^2 - n_{\mathrm{eff,THz}}^2}}\right). \quad (2)$$

According to Eq. (2), $n_{\mathrm{eff,THz}}$ can be changed by varying the thickness of planar waveguide to satisfy the phase-matching conditions between the m-th-order and the $(m+M)$-th-order cascaded optical waves to generate THz wave with frequency of $\omega_{\mathrm{T}M}$. In this work we take $\omega_{\mathrm{T1}} = 0.3$ THz for example.

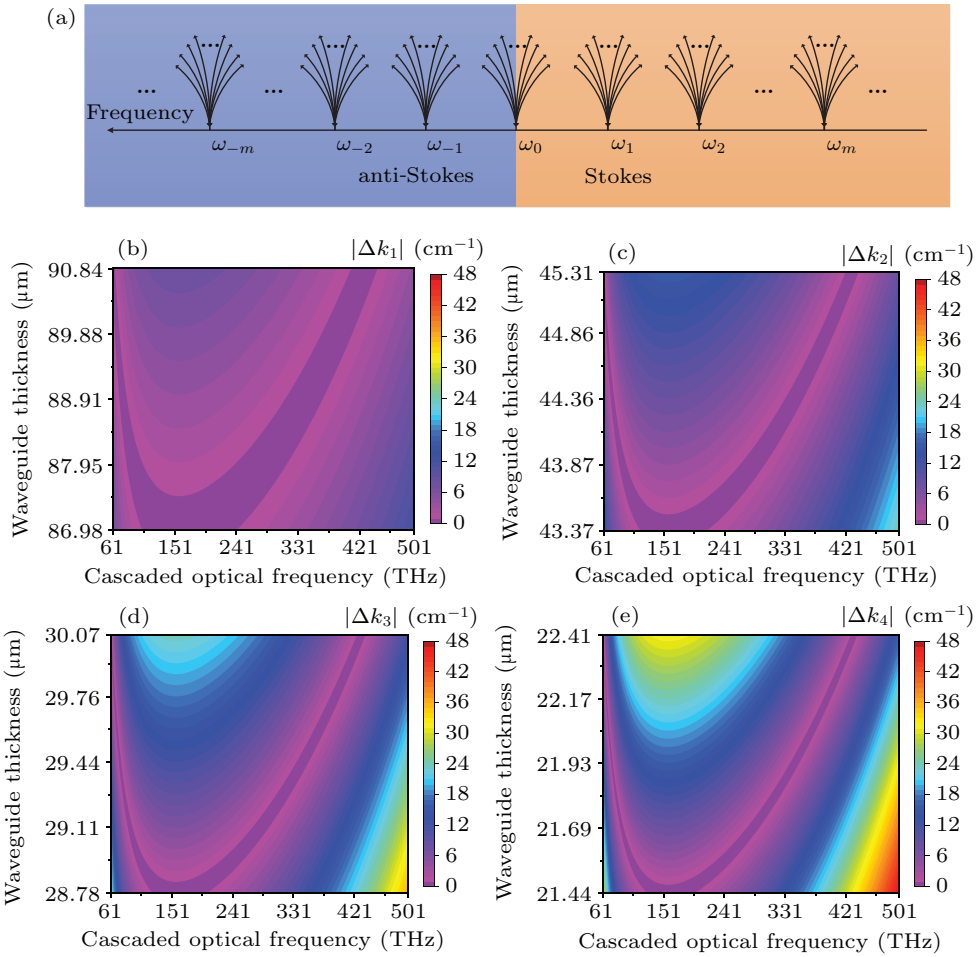


Fig. 1. Schematic diagram of OCDFG generating multi-frequency THz waves, showing (a) interactions between the m-th-order and the $(m+M)$-th-order cascaded optical waves, (b)–(f) waveguide thickness and phase mismatch $|\Delta k_M|$ *versus* the cascaded optical frequencies with $\omega_{\mathrm{T1}} = 0.3$ THz, $\omega_{\mathrm{T2}} = 0.6$ THz, $\omega_{\mathrm{T3}} = 0.9$ THz, and $\omega_{\mathrm{T4}} = 1.2$ THz, respectively.

Figures 1(b)–1(f) show the phase mismatch distributions of OCDFG generating 0.3 THz, 0.6 THz, 0.9 THz, and 1.2 THz, respectively. It can be seen from the figure that the greater the THz wave frequency, the larger the phase mismatches of OCDFG is. If the waveguide thickness t changes with the minimum phase mismatch of each order OCDFG from 291.76 THz to 61.36 THz, the phase mismatches in cascaded Stokes processes disappear one by one from the first-order Stokes process to high-order Stokes processes, and the phase mismatches in cascaded anti-Stokes processes increase as shown in Figs. 1(b)–1(f). The cascaded Stokes process is enhanced and the cascaded anti-Stokes process is suppressed simultaneously, resulting in the enhancement of THz wave intensity. The coupled wave equations of OCDFG are expressed as follows:

$$\frac{\mathrm{d}E_{\mathrm{TM}}}{\mathrm{d}z} = -\frac{\alpha_{\mathrm{TM}}}{2}E_{\mathrm{TM}} + \mathrm{j}\,\kappa_{\mathrm{TM}}\sum_{-\infty}^{+\infty} E_m E_{m+M}^{*}\,\mathrm{e}^{\mathrm{j}\Delta k_{(m)}z}, \quad (3)$$

$$\frac{\mathrm{d}E_m}{\mathrm{d}z} = -\frac{\alpha_m}{2}E_m + \mathrm{j}\,\kappa_m[E_{m-M}E_{\mathrm{TM}}^{*}\,\mathrm{e}^{\mathrm{j}\Delta k_{(m-M)}z} + E_{m+M}E_{\mathrm{TM}}\,\mathrm{e}^{-\mathrm{j}\Delta k_{(m)}z}], \quad (4)$$

$$\kappa_m = \frac{\Omega_m d_{\mathrm{eff}}}{c n_m}, \quad (5)$$

$$\kappa_{\mathrm{TM}} = \frac{\Omega_{\mathrm{TM}} d_{\mathrm{eff}}}{c n_{\mathrm{TM}}}, \quad (6)$$

$$\Delta k_{(m)} = k_m - k_{m+M} - k_{\mathrm{eff,THz}}, \tag{7}$$

$$I = \frac{1}{2} nc\varepsilon_0 |E|^2, \tag{8}$$

$$\eta(\omega_{\mathrm{TM}}, z) = \frac{n_{\mathrm{eff,THz}}(\omega_{\mathrm{TM}}) |E_{\mathrm{TM}}(\omega_{\mathrm{TM}}, z)|^2}{\sum n(\omega_m) |E_m(\omega_m, 0)|^2}, \tag{9}$$

where E is the electric field amplitude, the subscripts TM and m represent THz wave with M-times ω_{T1} and the m-th order cascaded optical wave, respectively, α denotes the absorption coefficient, κ is the coupling coefficient, Ω is the angular frequency, d_{eff} is the nonlinear coefficient, Δk is the phase mismatch, k is the wave vector in the waveguide, c is the speed of light in vacuum, I is the power density, ε_0 is the vacuum dielectric constant, and $\eta(\omega_{\mathrm{TM}}, z)$ corresponds to the energy conversion efficiency. On the right-hand side of Eq. (3), the first term corresponds to the THz wave absorption, and the second term corresponds to the sum of THz wave intensity generated by the OCDFG between ω_m and ω_{m+M}. On the right-hand side of Eq. (4), the first term corresponds to the absorption of cascaded optical waves, the second term corresponds to the enhancement of ω_m by the interaction between ω_{mM} and ω_{TM}, and the third term corresponds to the consumption of ω_m by the interaction between ω_{m+M} and ω_{TM}.

3. Calculations

In this section, the intensities of THz waves and the evolutions of cascaded optical waves are analyzed. The frequencies of the two incident lasers are 291.76 THz and 291.46 THz, respectively. $\omega_{\mathrm{T1}} = 0.3$ THz, $\omega_{\mathrm{T2}} = 0.6$ THz, $\omega_{\mathrm{T3}} = 0.9$ THz, and $\omega_{\mathrm{T4}} = 1.2$ THz. The intensities of the two incident lasers I_0 and I_1 are both 5 GW/cm^2. We use MgO:LiNbO$_3$ planar waveguide for analysis. The nonlinear coefficient of MgO:LiNbO$_3$ at 291.76 THz is 336 pm/V.[6] At 10 K, the THz wave absorption coefficients at 0.3 THz, 0.6 THz, 0.9 THz, and 1.2 THz in MgO:LiNbO$_3$ waveguide are 0.22 cm^{-1}, 0.25 cm^{-1}, 0.32 cm^{-1}, and 0.45 cm^{-1}, respectively. All the absorption coefficients of the cascaded optical waves are 0 cm^{-1}.[13] The laser damage threshold of MgO:LiNbO$_3$ with 100-ps pulse width is $\sim$ 10 GW/cm^2.[14] The theoretical values of the refractive index of MgO:LiNbO$_3$ in the infrared region[15] and THz region[13] are calculated by using the wavelength- and temperature-dependent Sellmeier equations, respectively. We set the cascaded optical frequency range to be 61.36 THz–500.56 THz. Figure 2 shows the THz wave intensities with $\omega_{\mathrm{T1}} = 0.3$ THz and the evolutions of cascaded optical spectra. It can be seen from Fig. 2(a) that the THz wave intensity monotonically increases, and the maximum intensity is 3.99 GW/cm^2 at $z = 9.7$ mm, corresponding to the energy conversion efficiency of 39.9%. As shown in Fig. 2(b), the thickness of waveguide first decreases and then increases with the waveguide length increasing, satisfying the phase matching conditions from the first order to higher order OCDFG, which is in accord with the variation trend in Fig. 1(b). Figure 2(c) shows the variation trend of cascaded optical spectra. The diffusion range of cascaded Stokes process is obviously larger than that of cascaded anti-Stokes process, which is in consistance with the increase trend of THz wave intensity in Fig. 2(a).

The generated THz wave intensity with $\omega_{\mathrm{T2}} = 0.6$ THz is shown in Fig. 3. The planar waveguide is divided into two parts. The THz wave with $\omega_{\mathrm{T1}} = 0.3$ THz and a series of cascaded optical waves are generated by OCDFG in the first part, while THz wave with $\omega_{\mathrm{T2}} = 0.6$ THz is generated by OCDFG in the second part. As shown in Fig. 3(a), in the first part from $z = 0$ mm to $z = 4$ mm, the THz wave intensity increases rapidly, which corresponds to the shaded part of Fig. 3(c). The THz wave with $\omega_{\mathrm{T1}} = 0.3$ THz cannot transmit in the second parts of the waveguide, so just the cascaded optical waves can enter into the second part of the waveguide. As shown in Fig. 3(b), the thickness variation of the first and the second parts of the waveguide satisfy the phase matching conditions of 0.3 THz and 0.6 THz from the first order to higher order OCDFG respectively, which is in accord with the variation trend in Figs. 1(b) and 1(c). The thickness variation of the second part leads the phase mismatches of OCDFG to be zero from the 1st order to the 350th order, and the maximum THz wave intensity reaches 2.37 GW/cm^2 at $z = 11.8$ mm, corresponding to the energy conversion efficiency of 23.7%. As shown in Fig. 3(c), by changing the waveguide thickness, the pump energy gradually transfers to high-order Stokes waves rather than high-order anti-Stokes waves.

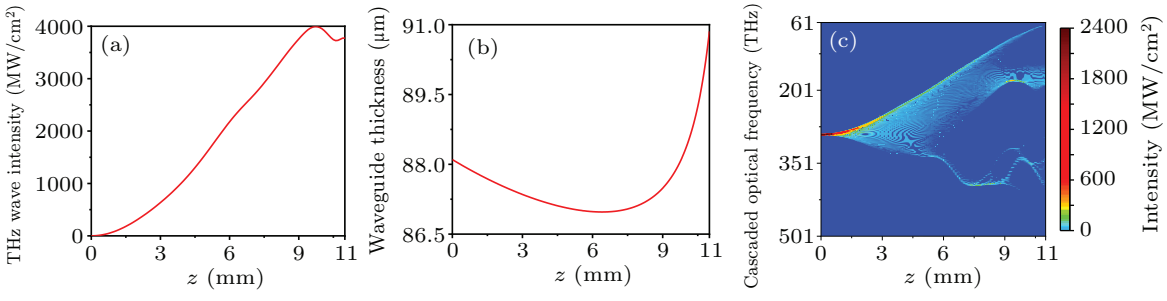


Fig. 2. THz wave intensities and thickness and the evolutions of cascaded optical spectra, $\omega_{\mathrm{T1}} = 0.3$ THz, $I_0 = I_1 = 5$ GW/cm^2, showing z-dependent (a) THz wave intensity, (b) waveguide thickness, and (c) cascaded optical spectra.

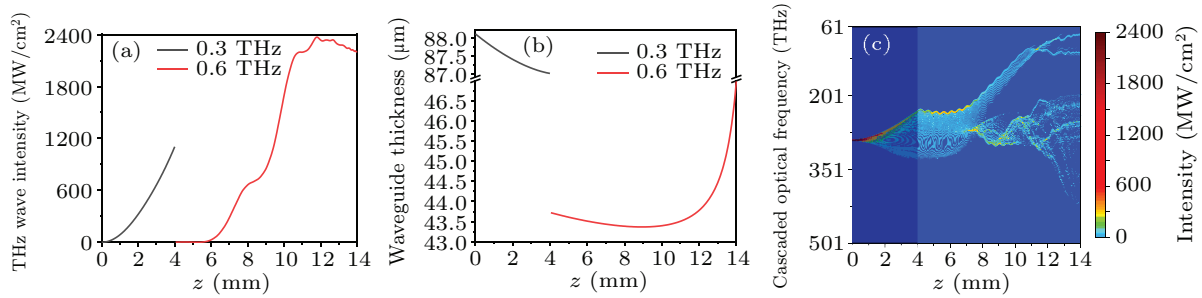


Fig. 3. THz wave intensities and thickness, and the evolutions of cascaded optical spectra, $\omega_{T1} = 0.3$ THz, $\omega_{T2} = 0.6$ THz, $I_0 = I_1 = 5$ GW/cm^2, showing z-dependent (a) THz wave intensities, (b) waveguide thickness, and (c) cascaded optical spectra.

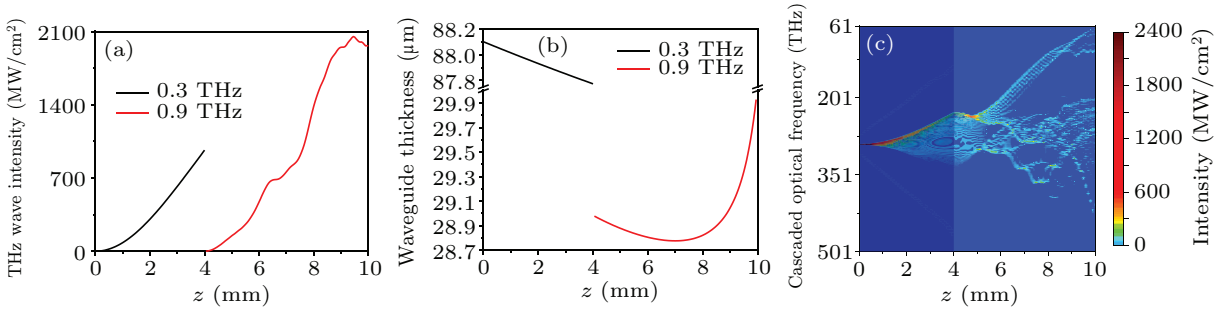


Fig. 4. THz wave intensities and thickness, and evolutions of cascaded optical spectra, $\omega_{T1} = 0.3$ THz, $\omega_{T3} = 0.9$ THz, $I_0 = I_1 = 5$ GW/cm^2, showing z-dependent (a) THz wave intensities, (b) waveguide thickness , and (c) cascaded optical spectra.

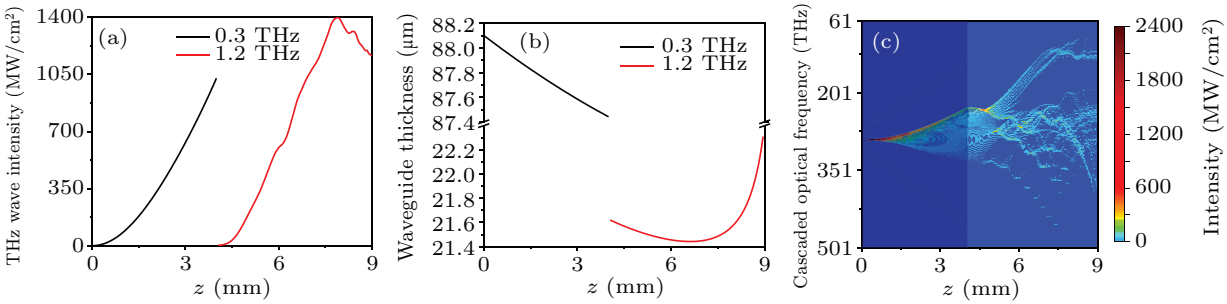


Fig. 5. THz wave intensities and thickness, and the evolutions of cascaded optical spectra, $\omega_{T1} = 0.3$ THz, $\omega_{T4} = 1.2$ THz, $I_0 = I_1 = 5$ GW/cm^2, showing z-dependent (a) THz wave intensities, (b) waveguide thickness, and (c) cascaded optical spectra.

The generated THz wave intensity with $\omega_{T3} = 0.9$ THz is shown in Fig. 4. It can be observed from Fig. 4(a) that in the first stage from $z = 0$ mm to $z = 4$ mm, THz wave intensity gradually increases. In order to effectively produce THz wave with a frequency of 0.9 THz, the phase mismatches between cascaded optical waves are zero from the 1st order to the 213th order by changing the waveguide thickness with $z > 4$ mm. The THz wave intensity rapidly increases, and the maximum THz wave intensity reaches 2.05 GW/cm^2 at $z = 9.45$ mm, corresponding to an energy conversion efficiency of 20.5%. The waveguide thickness values in the two parts, shown in Fig. 4(b), fulfill the phase-matching conditions between cascaded optical waves with frequency intervals of 0.3 THz and 0.9 THz, respectively. The variations of THz wave intensity are consistent with those of the cascaded optical spectra shown in Fig. 4(c) where more pump photons are transferred into high-order Stokes waves.

The THz wave generation with $\omega_{T4} = 1.2$ THz is shown in Fig. 5. As shown in Fig. 5(a), both of the THz wave intensities of 0.3 THz and 1.2 THz generated by OCDFG increase rapidly with z increasing. For $z > 4$ mm, the thickness of the second part of waveguide changes along the red curve in Fig. 5(b). The phase mismatch between the cascaded optical waves with an interval of 1.2 THz is zero from the 1st order to the 169th order. The THz wave intensity gradually increases with the waveguide length increasing, and it reaches a maximum value of 1.397 GW/cm^2 at $z = 7.9$ mm, corresponding to an energy conversion efficiency of 13.97%. Comparing with cascaded optical waves in Figs. 3(c) and 4(c), the diffusion range of cascaded optical waves in Stokes area is narrow in Fig. 5(c). As shown in Fig. 1(e), the phase mismatch of OCDFG is separately larger than that in Figs. 1(c) and 1(d), so the diffusion range in Fig. 5(c) is restricted, as a result, the THz wave intensity is depressed simultaneously.

As shown in Fig. 1(a), the cascaded optical waves with a frequency interval of 0.3 THz can generate 0.6 THz, 0.9 THz, and 1.2 THz one by one with four waveguides. The THz wave of 0.3 THz generated in the first waveguide is coupled

out by a quartz coupler and does not transmit into the second waveguide. Similarly, the THz waves of 0.6 THz, 0.9 THz, and 1.2 THz generated in the second, the third, and the fourth waveguides respectively are coupled out by a quartz coupler, and do transmit into the next waveguide. The cascaded optical waves transmit and interact with each other in all the four waveguides. The scheme discussed above has been proposed in Ref. [16]. Figure 6 shows THz wave generations of 0.3 THz, 0.6 THz, 0.9 THz, and 1.2 THz by OCDFG. The thickness variations of the four waveguides, as shown in Fig. 6(b), fulfill the phase-matching conditions among the cascaded optical waves with frequency intervals of 0.3 THz, 0.6 THz, 0.9 THz, and 1.2 THz, respectively. All the four THz wave intensities rapidly increase and reach the maximum value of 587.43 MW/cm^2 for 0.3 THz at $z = 3$ mm, 559.30 MW/cm^2 for 0.6 THz at $z = 9$ mm, 541.40 MW/cm^2 for 0.9 THz at $z = 11.7$ mm, and 582.06 MW/cm^2 for 1.2 THz at $z = 17.7$ mm, respectively. The evolution of cascaded optical waves is shown in Fig. 6(c). For each waveguide, the cascaded optical waves are gradually transferred into high-order Stokes waves. The intensities of the four THz waves can be adjusted by changing the waveguide thickness.

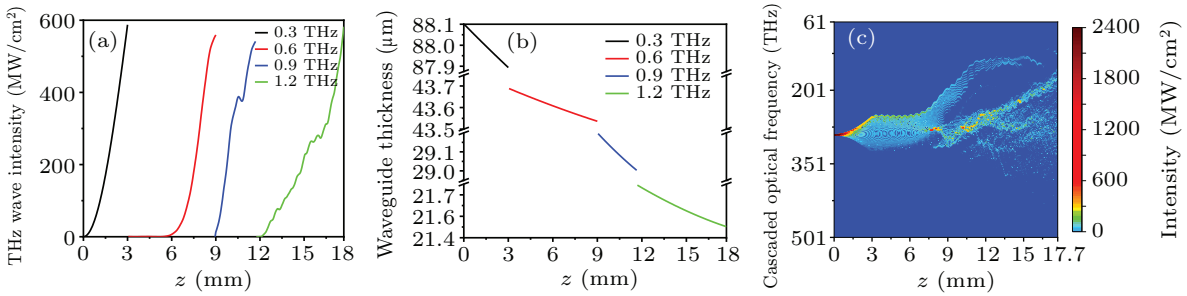


Fig. 6. THz wave intensities, thickness, and the evolutions of cascaded optical spectra, $\omega_{T1} = 0.3$ THz, $\omega_{T2} = 0.6$ THz, $\omega_{T3} = 0.9$ THz, $\omega_{T4} = 1.2$ THz, $I_0 = I_1 = 5$ GW/cm^2, showing z-dependent (a) THz wave intensities, (b) waveguide thickness t, and (c) cascaded optical spectra.

The waveguides with several tens of microns in this work can be fabricated with extreme ultraviolet lithography and inductively coupled plasma etching. The waveguides with gradually changing thickness have been extensively utilized in Refs. [17–19]. However, it is a tough task to simultaneously couple the cascaded optical waves into the waveguides because the cascaded optical waves exhibit different propagation constants. Moreover, it is extremely difficult to keep the cascaded optical waves propagating without walk-off when the THz wave is coupled out by the quartz coupler because the cascaded optical waves have distinct dispersion characteristics.

4. Conclusions

We proposed a scheme to generate multi-frequency THz waves by OCDFG through using an MgO:LiNbO$_3$ planar waveguide at 10 K. By optimizing the waveguide thickness, the m-th-order optical wave can interact with the $(m+M)$-th-order optical wave generating THz wave with multi-frequencies. The intensities of multi-frequency THz waves can be enhanced by modulating the phase mismatch distributions of CDFG. When the intensities of the two incident lasers are both 5 GW/cm^2, the THz wave intensity of 587.43 MW/cm^2 for 0.3 THz, 559.30 MW/cm^2 for 0.6 THz, 541.40 MW/cm^2 for 0.9 THz, and 582.06 MW/cm^2 for 1.2 THz are realized by OCDFG, respectively. The effective scheme in this work provides an option for generating the high-power pulsed or quasi-continuous THz waves.

Acknowledgements

Project supported by the National Natural Science Foundation of China (Grant Nos. 61735010, 31671580, and 61601183), the Natural Science Foundation of Henan Province, China (Grant No. 162300410190), and the Program for Science & Technology Innovation Talents in Universities of Henan Province, China (Grant No. 18HASTIT023).

References

[1] Baker C, Lo T, Tribe W R, Cole B E, Hogbin M R and Kemp M C 2007 *Proc. IEEE Inst. Electr. Electron Eng.* **95** 1559
[2] Liang M Y, Zhang C L, Zhao R and Zhao Y J 2014 *J. Infrared, Millimeter, Terahertz Waves* **35** 780
[3] Jepsen P U, Cooke D G and Koch M 2011 *Laser Photon. Rev.* **5** 124
[4] Dong J, Jackson J B, Melis M, Giovanacci D, Walker G C, Locquet A, Bowen J W and Citrin D S 2016 *Opt. Express* **24** 26972
[5] Liu P, Xu D, Yu H, Zhang H, Li Z, Zhong K, Wang Y and Yao J Q 2013 *J. Light. Technol.* **31** 2508
[6] Ravi K, Schimpf D N and Kärtner F X 2016 *Opt. Express* **24** 25582
[7] Saito K, Tanabe T and Oyama Y 2015 *J. Opt. Soc. Am. B* **32** 617
[8] Kiessling J, Sowade R, Breunig I, Buse K and Dierolf V 2009 *Opt. Express* **17** 87
[9] Li Z Y, Sun X Q, Li Y J, Yuan B, Zhang H T, Bing P B, Wang Z and Yao J Q 2020 *Opt. Lasers Eng.* **128** 106035
[10] Hu C F, Zhong K, Mei J L, Wang M R, Guo S B, Xu W Z, Liu P X, Xu D G, Wang Y Y and Yao J Q 2015 *Mod. Phys. Lett. B* **29** 1
[11] Ravi K and Kärtner F X 2020 *Laser Photon. Rev.* **14** 6
[12] Saito K, Tanabe T and Oyama Y 2012 *Opt. Express* **20** 26082
[13] Pálfalvi L, Hebling J, Kuhl J, Péterá and Polgár K 2005 *J. Appl. Phys.* **97** 123505
[14] Carbajo S, Stanford Linear Accelerator Center, 2575 Sand Hill Road, Menlo Park, CA 9402 (personal communication, 2015)
[15] Jundt D H 1997 *Opt. Lett.* **22** 1553
[16] Wang L, Fallahi A, Ravi K and Kärtner F 2018 *Opt. Express* **26** 29744
[17] Tan Y, Wu H, Wang S, Li C and Dai D 2018 *Opt. Lett.* **43** 1962
[18] Zheng S, Huang M, Cao X, Wang L, Ruan Z, Shen L and Wang J 2019 *Photon. Res.* **7** 1030
[19] Dai D 2017 *J. Light. Technol.* **35** 572